Korean J. Chem. Eng., **30**(9), 1691-1699 (2013)
DOI: 10.1007/s11814-013-0123-7

An explicit solution of the mathematical model for osmotic desalination process

Do Yeon Kim, Boram Gu, and Dae Ryook Yang†

Department of Chemical and Biological Engineering, Korea University, Anam-dong 5-Ga, Seongbuk-gu, Seoul 136-701, Korea
(*Received 6 May 2013 • accepted 9 July 2013*)

Abstract−Membrane processes such as reverse osmosis and forward osmosis for seawater desalination have gained attention in recent years. Mathematical models have been used to interpret the mechanism of membrane processes. The membrane process model, consisting of flux and concentration polarization (CP) models, is coupled with balance equations and solved simultaneously. This set of model equations is, however, implicit and nonlinear; consequently, the model must be solved iteratively and numerically, which is time- and cost-intensive. We suggest a method to transform implicit equations to their explicit form, in order to avoid an iterative procedure. In addition, the performance of five solving methods, including the method that we suggest, is tested and compared for accuracy, computation time, and robustness based on input conditions. Our proposed method shows the best performance based on the robustness of various simulation conditions, accuracy, and a cost-effective computation time.

Key words: Modeling, Desalination, Reverse Osmosis, Forward Osmosis, Membrane Process

INTRODUCTION

Membrane processes such as reverse osmosis (RO), and forward osmosis (FO) for seawater desalination have gained attention in recent years. Currently, RO is the most prevalent process for seawater desalination, and FO is regarded as cutting-edge technology. In such settings, mathematical models have been utilized to interpret the mechanism of membrane processes. There are several water and salt flux models available in the literature [1-4]; among these models, the solution-diffusion model developed by Merten [1] is the most commonly used. An important phenomenon that must be considered in a membrane process is concentration polarization (CP), induced by selectivity, permeability and an asymmetric structure of the membrane [11-20]. The mathematical model for CP is generally derived using the modified film theory [5]. The membrane process model, which consists of the flux and the CP model is coupled with balance equations and solved simultaneously. The set of model equations is, however, implicit and nonlinear; consequently, the model must be solved iteratively and numerically [6-8,11,13]. Even though there are many simulation studies on membrane processes available in literature, studies regarding solving techniques are limited. Zhou et al. [11] published a numerical study on CP and permeate flux in the RO process, in which they divided the channel into small segments and used integration via the Euler method. The water flux at the first segment was calculated by neglecting CP. From the second to the final segment, however, the polarized concentration was calculated using water flux at the previous segment, and subsequently, calculating water flux at the current segment again. Using this procedure, iterations were avoided in calculating water flux. However, the solution from this method showed high errors compared to the analytical solution, because of the accumulation of errors in integration. In addition, under extreme input conditions, the results display an oscillatory behavior, ultimately failing to converge. Another example of this is the lumped model, which uses an average value and empirical relations of operating variables; this method too gives poor predictions under various operating conditions.

Here, we suggest a method to transform implicit equations to their explicit form, in order to avoid the iterative procedure. In addition, the performance of five solving methods, including the method that we suggest, is tested and compared for accuracy, computation time, and robustness based on input conditions. Our proposed method shows the best performance based on the robustness of various simulation conditions, accuracy, and a cost-effective computation time.

METHODS

1. Theoretical Background

In RO and FO processes, the driving force for water permeation is expressed as the difference between hydraulic and osmotic pressures of the two channels divided by the membrane. Fig. 1 is a schematic of the driving force, and the direction of water and salt fluxes in RO and FO processes. In the RO process, a hydraulic pressure

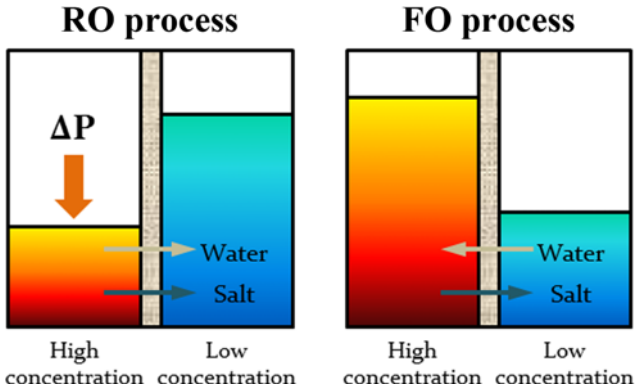

Fig. 1. Driving force and flux direction in RO and FO processes.

†To whom correspondence should be addressed.
E-mail: dryang@korea.ac.kr

greater than the osmotic pressure of seawater is applied to the seawater, so that water permeates from seawater to fresh water by hydraulic pressure. On the other hand, a draw solution, the osmotic pressure of which is higher than that of seawater, is introduced in a channel opposite to the seawater channel, so that the water in seawater is driven to the draw solution, owing to the difference in osmotic pressures.

The water and salt flux through the membrane can be expressed as a proportionality of the difference in osmotic and hydraulic pressures as follows:

$$J_w = \pm A(\Delta P - \Delta\pi_m) \quad (1)$$

$$J_s = \pm B\Delta C_m \quad (2)$$

where J_w is the water flux, J_s is the salt flux, A is the water permeability, B is the salt permeability, C_m is the concentration on the membrane surface, and ΔP and $\Delta\pi$ are the differences of hydraulic, and osmotic pressures, respectively, between the two solutions (i.e., seawater and fresh water in RO, and draw solution and seawater in FO). In Eqs. (1) and (2), both signs are positive in the RO process, negative in the FO process.

The osmotic pressure can be expressed as follows:

$$\pi = \alpha C \quad (3)$$

Concentration polarization phenomena are very important owing to their effect on flux reduction. Therefore, the difference in osmotic pressures, $\Delta\pi$, and the difference in concentrations, ΔC, in Eqs. (1) and (2) should be modified with respect to concentration polarization. Using an asymmetric membrane, the CP phenomenon can be classified as either external or internal concentration polarization (ECP and ICP), occurring in different locations of the membrane. ECP takes place on the active layer of the membrane, whereas ICP occurs inside the support layer of the membrane.

In the RO process, the ICP may be ignored, because virtually pure water meets the support layer of membrane; consequently, the gradient of concentration inside the support layer may be neglected.

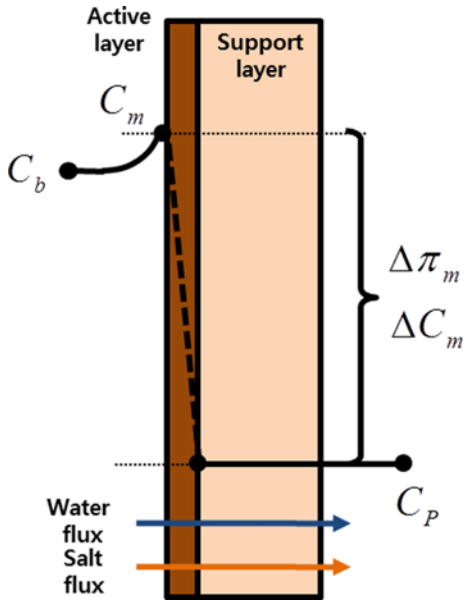

Fig. 2. Concentration profile for the RO process.

Fig. 2 shows the concentration profile through the membrane in the RO process. The ECP is expressed as a ratio of concentrations on the bulk side and on the membrane surface, derived from the boundary layer film theory, as follows [11-16]:

$$\frac{C_m}{C_b} = \exp\left(\frac{J_w}{k}\right) \quad (4)$$

where k is the mass transfer coefficient, and C_b and C_m are the concentrations on the bulk side and on the membrane surface, respectively. The mass transfer coefficient k may be correlated with the Sherwood number, which is empirically expressed using the Reynolds number Re and the Schmidt number Sc as follows:

$$k = \frac{Sh \cdot D}{d_h} \quad (5)$$

$$Sh = \kappa Re^{\beta} Sc^{\gamma} \quad (6)$$

On the other hand, both ECP and ICP should be considered in the FO process, unlike in the RO process. ICP ensues inside the porous support layer of the membrane, and thus, it is not affected by the characteristics of fluid flow in the channel, in contrast to ECP. ICP may be derived as follows:

$$-J_s = B(C_{D,m} - C_{F,m}) = D\varepsilon\frac{dC(x)}{dx} - J_w C(x) \quad (7)$$

where D is the diffusivity and ε is the porosity of the support layer. Two different cases may result, according to the orientation of the asymmetric membrane. One is when the active layer meets the draw solution (AL-DS), and the other is when the active layer meets the feed solution (AL-FW). Fig. 3 shows the concentration profiles of both cases. The boundary conditions for Eq. (7) are shown in Eqs. (8) and (9) in each case, as follows:

$$\text{B.C. } C(x) = C_{F,b} \text{ at } x = 0;\quad C(x) = C_{F,m} \text{ at } x = \tau t \quad \text{(AL-DS)} \quad (8)$$

$$\text{B.C. } C(x) = C_{D,m} \text{ at } x = 0;\quad C(x) = C_{D,b} \text{ at } x = \tau t \quad \text{(AL-FW)} \quad (9)$$

where t is the thickness and τ the tortuosity of the support layer. By integration of the ordinary differential Eq. (7), using these boundary

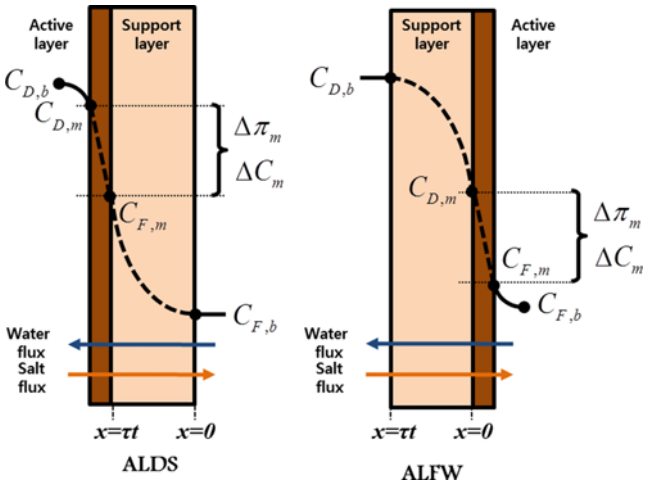

Fig. 3. Concentration profile for the FO process.

conditions the following equations are obtained [17-20]:

$$C_{D,m}=\exp\left(-\frac{J_w}{k}\right) \quad \text{: Dilutive ECP (AL-DS)} \quad (10)$$

$$C_{F,m}=C_{D,m}-\frac{C_{D,m}-C_{F,b}\exp(J_wK)}{1+\frac{B}{J_w}[\exp(J_wK)-1]} \quad \text{: Concentrative ICP}$$

$$C_{F,m}=\exp\left(\frac{J_w}{k}\right) \quad \text{: Concentrative ECP (AL-DS)} \quad (11)$$

$$C_{D,m}=C_{F,m}-\frac{C_{F,m}-C_{D,b}\exp(-J_wK)}{1-\frac{B}{J_w}[\exp(-J_wK)-1]} \quad \text{: Dilutive ICP}$$

$$K=\frac{\tau t}{D\varepsilon} \quad (12)$$

where K is the resistivity within the support layer.

To calculate the water and salt fluxes in the RO process, Eqs. (1)-(6) are used; in the FO process, Eqs. (10)-(12) are additionally required. The concentrations on the membrane surface and the interface between the active layer and the support layer are required to calculate water flux J_w in Eq. (1), when both CPs are considered. However, the water flux is also needed to calculate these concentrations; i.e., the combined water flux equation, with equations of CPs is implicit. Therefore, an iterative procedure is necessary for an accurate solution. However, techniques to solve implicit equations usually require high computation times. In the next section, a method for transforming the implicit form of these equations to their explicit form, for water flux calculations, is shown to avoid an iterative procedure.

2. Transformation to Explicit Form

The existence of an exponential function in the model is the reason for the flux model with CP being implicit; therefore, the exponential function was substituted with a second-order polynomial, to transform the implicit equation to an explicit one. The exponential terms for concentrative and dilutive CP were approximated as shown in Eqs. (13) and (14), respectively:

$$\exp(X)\simeq a_+X^2+b_+X+1 \text{ (For concentrative CP)} \quad (13)$$

$$\exp(-X)\simeq a_-X^2+b_-X+1 \text{ (For dilutive CP)} \quad (14)$$

In the flux model, the exponential term implies the ratio of the concentration on the membrane induced by CP, to the concentration in the bulk side. For both concentrative and dilutive CP, the ratio of higher concentration (C_m for concentrative CP and C_b for dilutive CP) to lower concentration (C_b for concentrative CP and C_m for dilutive CP) was found to barely exceed a factor of 1.5; i.e., in case of concentrative CP, the value of the exponential term was <1.7, and in case of dilutive CP, it was >0.6. In this study, the independent variable X in Eqs. (13) and (14) was selected to range from 0 to 0.6, to satisfy operation and design conditions.

The coefficients of the second-order polynomial in Eqs. (13) and (14) were identified by minimizing the sum of errors between the exponential and the second-order polynomial function in the range of 0 to 0.6; identified coefficients are listed in Table 1. Figs. 4 and 5 show the exponential function, and the approximated second order polynomial function as expressed in Eqs. (13) and (14), respectively. An error within 0.5% was seen in the chosen range of the independent variable, X; thus, the flux equations for the RO and FO processes were constituted using a second-order polynomial equation, making it easy to obtain water flux by using the quadratic formula.

2-1. The RO Process

In the RO process, Eq. (4) for ECP was converted into Eq. (15) by introducing a second polynomial function in Eq. (13).

$$C_m=\left(a_+\left(\frac{J_w}{k}\right)^2+b_+\left(\frac{J_w}{k}\right)+1\right)C_b \quad (15)$$

By substituting C_m from Eq. (15) into Eqs. (1) and (3), the following second-order polynomial was obtained as a function of J_w:

$$a'J_w^2+b'J_w+c'=0$$
$$\text{where } a'=\frac{A}{k^3}\alpha C_b a_+,\ b'=\frac{A}{k^2}\alpha C_b b_++\frac{1}{k},\ c'=-\frac{A}{k}(\Delta p-\alpha C_b) \quad (16)$$

Table 1. Coefficients of second polynomial equations

	a_+/a_-	b_+/b_-
exp(X)	0.6577	0.9700
exp(−X)	0.3857	−0.9805

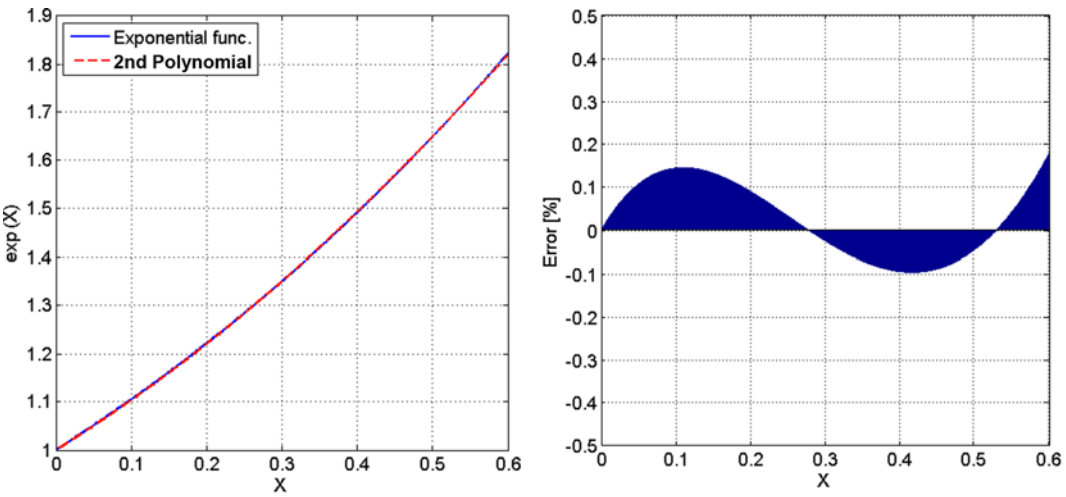

Fig. 4. Comparison of exp(x) and second polynomial function.

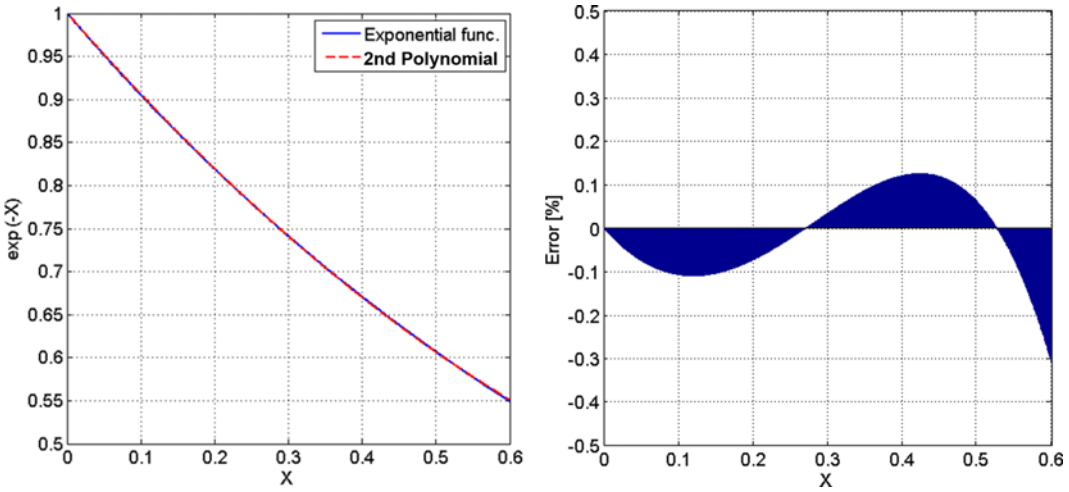

Fig. 5. Comparison of exp(−x) and second polynomial function.

Because J_w is positive, only a single root value is possible for Eq. (16). The water flux calculated using the quadratic formula is as follows:

$$J_w = \frac{-b' + \sqrt{b'^2 - 4a'c'}}{2a'} \tag{17}$$

Using the calculated J_w, the concentration on the membrane surface may be calculated, and the salt flux may subsequently be calculated using Eq. (2).

2-2. The FO Process

The second-order polynomial equation in the FO process was constituted using a similar procedure as in the RO process as explained previously. However, because of the asymmetric membrane, the conversion of the flux equation must be conducted separately.

In the AL-DS mode, Eqs. (13) and (14) were used, respectively, to substitute the exponential terms in the concentrative ICP and dilutive ECP in Eq. (10). As a result, the concentration difference is expressed in the form of the second-order Eq. (18):

$$\Delta C_m = C_{D,m} - C_{F,m} = \frac{C_{D,b}\left[a_-\left(\frac{J_w}{k}\right)^2 + b_-\left(\frac{J_w}{k}\right) + 1\right] - C_{F,b}[a_+(J_wK)^2 + b_+(J_wK) + 1]}{1 + \frac{B}{J_w}[a_+(J_wK)^2 + b_+(J_wK)]} \tag{18}$$

Eq. (18) was substituted into Eqs. (1) and (3); consequently, the following second-order polynomial equation was obtained to calculate J_w.

$$(A\alpha a' - b'')J_w^2 + (A\alpha b' - c'' - A\Delta pb'')J_w + (A\alpha c' - A\Delta pc'') = 0$$
$$\text{where } a' = \left(\frac{C_{D,b}a_-}{k^2} - C_{F,b}a_+K^2\right),\ b' = \left(\frac{C_{D,b}b_-}{k} - C_{F,b}b_+K\right),$$
$$c' = (C_{D,b} - C_{F,b})$$
$$b'' = (Ba_+K^2),\ c'' = (Bb_+K + 1) \tag{19}$$

However, unlike in the RO process, it is difficult to estimate which root value is an actual solution between the two roots from the quadratic formula, by investigating the coefficients in Eq. (19) alone. Thus, to obtain the appropriate formula that gives the actual solution, the FO process was simulated in a broad range of operating conditions, and the values calculated from the quadratic formula were checked. It was found that the quadratic formula with the negative sign produces the actual solution in most trials. Thus, J_w is expressed as follows:

$$J_w = \frac{-(A\alpha b' - c'' - A\Delta pb'') - \sqrt{(A\alpha b' - c'' - A\Delta pb'')^2 - 4(A\alpha a' - b'')(A\alpha c' - A\Delta pc'')}}{2(A\alpha a' - b'')} \tag{20}$$

In the AL-FW mode, Eq. (11) was converted into the following equation by considering concentrative ECP and dilutive ICP:

$$\Delta C_m = C_{D,m} - C_{F,m} = \frac{C_{D,b}\left[a_-\left(\frac{J_w}{k}\right)^2 + b_-\left(\frac{J_w}{k}\right) + 1\right] - C_{D,b}[a_-(J_wK)^2 + b_-(J_wK) + 1]}{1 - \frac{B}{J_w}[a_-(J_wK)^2 + b_-(J_wK)]} \tag{21}$$

The second-order polynomial equation for AL-FW mode is as follows:

$$(A\alpha a' - b'')J_w^2 + (A\alpha b' - c'' - A\Delta pb'')J_w + (A\alpha c' - A\Delta pc'') = 0$$
$$\text{where } a' = \left(C_{F,b}\frac{a_+}{k^2} - C_{D,b}a_-K^2\right),\ b' = \left(C_{F,b}\frac{b_+}{k} - C_{D,b}b_-K\right),$$
$$c' = (C_{F,b} - C_{D,b})$$
$$b'' = (Ba_-K^2),\ c'' = (Bb_-K - 1) \tag{22}$$

As in the case of the AL-DS mode, J_w in the AL-FW mode was also calculated using Eq. (20).

3. Modeling and Numerical Procedure

A membrane module constructed using a flat sheet membrane is used commonly in both RO and FO processes. The overall and component mass balance equations of the flat sheet membrane module in the RO process may be derived as follows:

$$\frac{du_f}{dx} = -\frac{J_w}{H}$$
$$\frac{dC}{dx} = -\frac{J_s}{u_f H} + \frac{CJ_w}{u_f H} \tag{23}$$

where H is the channel height and u is the axial velocity of the solution.

In the FO process, there are two inlet streams: feed seawater and

draw solution. Therefore, two sets of mass balance equations exist, and they may be expressed as follows:

[feed seawater side]

$$\frac{du_f}{dx} = -\frac{J_w}{H}$$
$$\frac{dC}{dx} = \frac{J_s}{u_f H} + \frac{CJ_w}{u_f H} \quad (24)$$

[draw solution side]

$$\frac{du_d}{dx} = \frac{J_w}{H}$$
$$\frac{dC}{dx} = -\frac{J_s}{u_d H} - \frac{CJ_w}{u_d H} \quad (25)$$

These mass balance equations may be simplified using several assumptions such as neglecting the molecular volume of solutes and assuming that the natural diffusion in the channel is negligible compared to forced convection. As the solution flows along the channel, its pressure decreases owing to flow friction with channel walls and spacers. This pressure drop may be calculated as follows:

$$\frac{dP}{dx} = -k_f \frac{\mu}{H^2} u \quad (26)$$

where k_f is the friction coefficient due to the existence of spacers and other irregularities, and μ is the viscosity of the solution.

To simulate the RO and FO processes, the set of the equations consisting of flux, mass balance, and pressure drop must be solved simultaneously. When the flux model includes exponential terms, the set of the equations must be solved iteratively owing to its implicit characteristics. The iterative procedure for solving the set of equation is shown in Fig. 6. On the other hand, when the flux model is converted into its explicit form by approximating the exponential function to a second-order polynomial function, the set of the equations consisting of ordinary differential and algebraic equations may be simply solved without using the iterative procedure.

RESULTS AND DISCUSSION

The performance of the following five solving methods were tested and compared:

Method 1: The 4th order Runge-Kutta method for mass balance/pressure drop equations, and an iterative procedure for the flux model (no approximation of exponential terms)

Method 2: The 4th order Runge-Kutta method for mass balance/pressure drop equations, and a 2nd order polynomial approximation for the flux model

Method 3: The Euler method for mass balance/pressure drop equations, and considering the water flux of previous segment for current segment calculations (as described previously [6])

Method 4: The Euler method for mass balance/pressure drop equations, and an iterative procedure for the flux model

Method 5: The Euler method for mass balance/pressure drop equations, and a 2nd order polynomial approximation for the flux model

To test the five methods, all programs were coded using MATLAB. The built-in function, "ode45", was used for the 4th order Runge-Kutta method, and the Euler method was hand-programmed with a sufficient number of discretized segments [21,22]. The Wegstein method was introduced to calculate water flux as an iterative procedure. In Method 3, the water flux at the first segment was calculated using an iterative procedure in the Wegstein method, in order

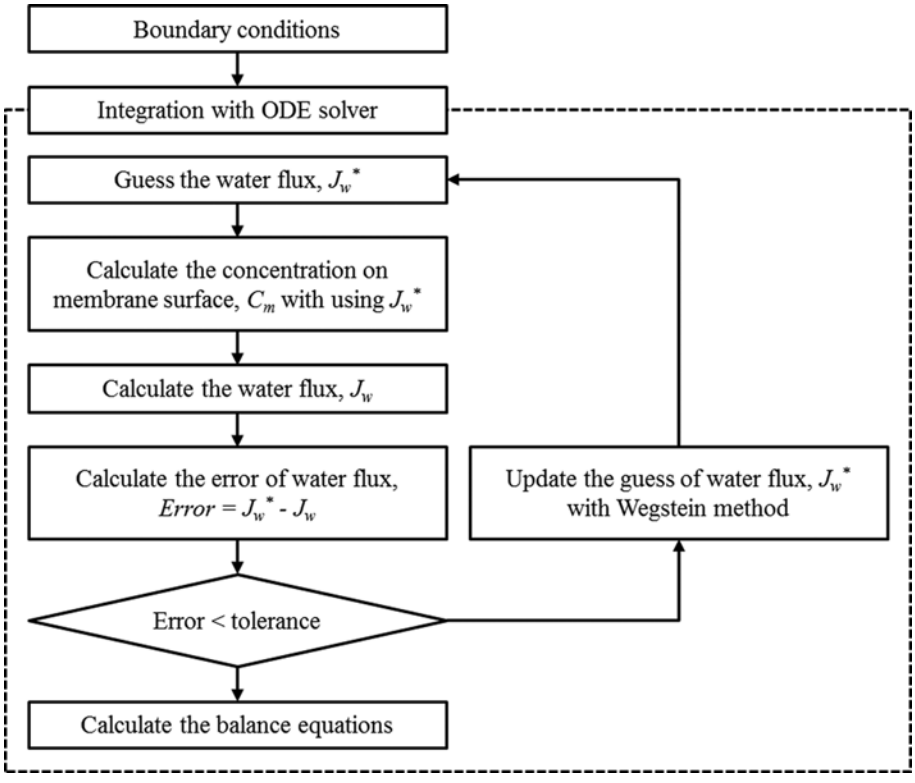

Fig. 6. Algorithm of the iterative procedure for solving the set of equations.

Table 2. Values of input variables to simulate RO and FO processes

		RO process	FO process
Water permeation coefficient, A [m/s Pa]		4.7010E-12	2.7350E-12
Salt permeation coefficient, B [m/s]		3.7908E-08	7.1213E-08
Membrane module	Length [m]	7.112	7.112
	Area [m^2]	26,040	26,040
Feed seawater	Flow rate [m^3/day]	25,678	25,678
	Pressure [bar]	60.00	1.56
	Concentration [kg/m^3]	36	36
Draw solution	Flow rate [m^3/day]	-	25,678
	Pressure [bar]	-	1.80
	Concentration [kg/m^3]	-	100

to avoid a large discrepancy compared to the analytical solution at the starting point [23]. A comparison of performances was conducted with respect to accuracy, computation time, and robustness based on input conditions. The solution obtained from the Method 1 was found to be the closest to the actual solution; hence, accuracy was tested based on the solution from the Method 1. The computation time was measured for each method under the same conditions, and using the same computer (CPU clock: quad core 3.5 GHz, Memory: 8.00 GB). For a test of robustness, four cases of extreme operating and design conditions were used.

1. Accuracy Test

As shown in Table 2, the operating and design conditions for the accuracy test were selected to satisfy the capacity of approximately 10,000 tons/day. In the RO process, the pressure at the permeate side is set to 1 bar and the feed velocity is about 0.19 m/s. The coefficients A and B in both processes were arbitrarily selected based on the characteristics of commercial membranes. The feed seawater and draw solution were assumed to be aqueous sodium chloride solutions.

1-1. The RO Process

The simulation results using the five different methods and their errors compared to Method 1 are listed in Table 3. Of the four methods, Method 2, i.e., conversion into the explicit form, was found to show the least error in the permeate flow rate, pressure drop, and permeate concentration. In Methods 4 and 5, the errors in concentration were considerably high (≈12%), while the errors in other values were low (<0.2%). Methods 4 and 5 show much higher errors than Method 2 because the Euler method was used to solve ordinary differential equations. Method 3 performed the worst in the accuracy test, with errors greater than 10% in the values of permeate flow rate, and permeate concentration, and approximately 3% in pressure drop; this is because of the errors in water flux caused by the approximation accumulate along the length direction.

Fig. 7 illustrates the simulation results of concentration, feed velocity, pressure, and permeate flux along the flow direction. The lines of all methods, except Method 3, were found to overlap. At the beginning of the module, there was no discrepancy among the five methods; however, as the feed flows along the length direction, the line for Method 3 was found to deviate conspicuously from the others, owing to the accumulation of errors.

1-2. The FO Process

In the FO process, all four methods resulted in low errors of within 0.3%; Method 4 showed the highest accuracy and Method 3 the lowest. Compared to the RO process, the errors were lower because the water flux in FO is half of that in RO. As shown in Table 4, in the simulation results of Method 4, the numerical errors using the Euler method are lower compared to the results of the RO process, because the water flux along the flow direction has lower non-linearity than in the RO process. In Method 2, the error results from the approximation of exponential terms. Fig. 8 shows the results of all five methods. All lines overlap because of low errors.

Using the accuracy test, it was concluded that Methods 2, 4, and 5, but not Method 3, display a satisfactory accuracy.

2. Computation Time Test

The computation time test was conducted by measuring time for the following two cases: a single simulation and 100 consecutive simulations. The computation time of the single simulation was averaged over twenty single simulations. Consecutive simulations were aimed to examine the performance in case of optimization and identifications that require numerous calculations.

The order among the five methods based on rapidness of computation is as follows: Method 2, 1, 3, 5, and 4. Compared to Method 1, Method 2 showed only a 2% reduction in time, despite the absence of the iterative procedure owing to the approximation. Methods 3, 4, and 5 using the Euler method took longer for computation because they require a larger number of segments in order to satisfy the accuracy criterion.

3. Robustness Test

Four cases each for the RO and FO process were used to conduct the robustness test, and were selected by combining two extreme operating conditions: feed flow rate, and driving force. The operating conditions are listed in Table 6.

Table 3. Simulation results of the RO process using five different methods and their errors

		Method 1	Method 2	Method 3	Method 4	Method 5
Permeate	Value [m^3/day]	11193.27	11200.34	10007.82	11205.45	11212.53
	Error [%]	-	−0.06	10.59	−0.11	−0.17
Pressure drop	Value [bar]	2.42	2.42	2.49	2.42	2.42
	Error [%]	-	0.00	−2.89	0.00	0.00
Concentration	Value [mg/L]	416.44	416.13	476.85	465.83	465.62
	Error [%]	-	0.07	−14.51	−11.86	−11.81
Recovery	Value [%]	43.59	43.62	38.97	43.64	43.67
	Error [%]	-	−0.07	10.60	−0.11	−0.18

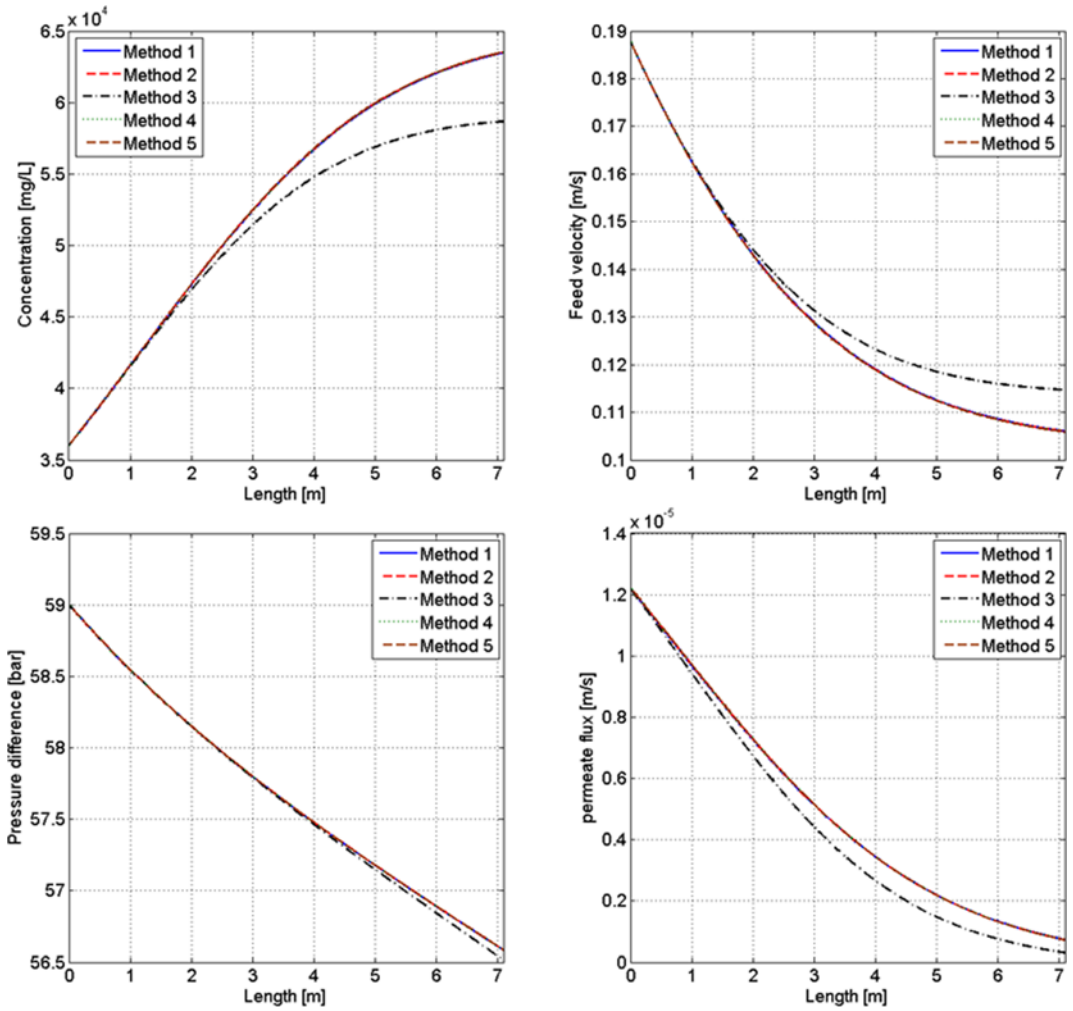

Fig. 7. Simulation results of the RO process along the flow direction.

Table 4. Simulation results of the FO process using the five different methods and their errors

		Method 1	Method 2	Method 3	Method 4	Method 5
Permeate	Value [m^3/day]	9094.39	9102.96	9069.52	9097.29	9105.85
	Error [%]	-	−0.09	0.27	−0.03	−0.13
Pressure drop	Value [bar]	0.54	0.54	0.54	0.54	0.54
	Error [%]	-	0.0	0.0	0.0	0.0
Concentration	Value [ppm]	55912.31	55941.38	55813.64	55906.32	55935.35
	Error [%]	-	−0.05	0.18	0.01	−0.04
Recovery	Value [%]	35.42	35.45	35.32	35.43	35.46
	Error [%]	-	−0.08	0.28	−0.03	−0.11

3-1. The RO Process

The simulation results for the robustness test are shown in Table 7, where "Success" indicates convergence of the simulation, and "Fail" indicates failure in convergence. Methods 1 and 4 that use the iterative procedure i.e., the Wegstein method, failed to converge in case of low axial velocity and high driving force, because the water flux calculation diverges in the iterative procedure.

3-2. The FO Process

Similar to the results of the RO process, Methods 1 and 4 failed to converge in case of low axial velocity and high driving force. Method 3 also failed to converge in three cases, because of oscillations in the water flux, as depicted in Fig. 9; therefore, the approximation used in Method 3 may be unreasonable.

The following is a summary of the performance tests:

1. Method 1 shows the highest accuracy; however, its robustness of convergence under various operating conditions is unsatisfactory.

2. Method 2 shows the lowest errors in accuracy (except compared to Method 1), the most rapid computation time, and is highly robust.

3. Method 3 shows a poor accuracy, moderate computation speed, and is the least robust.

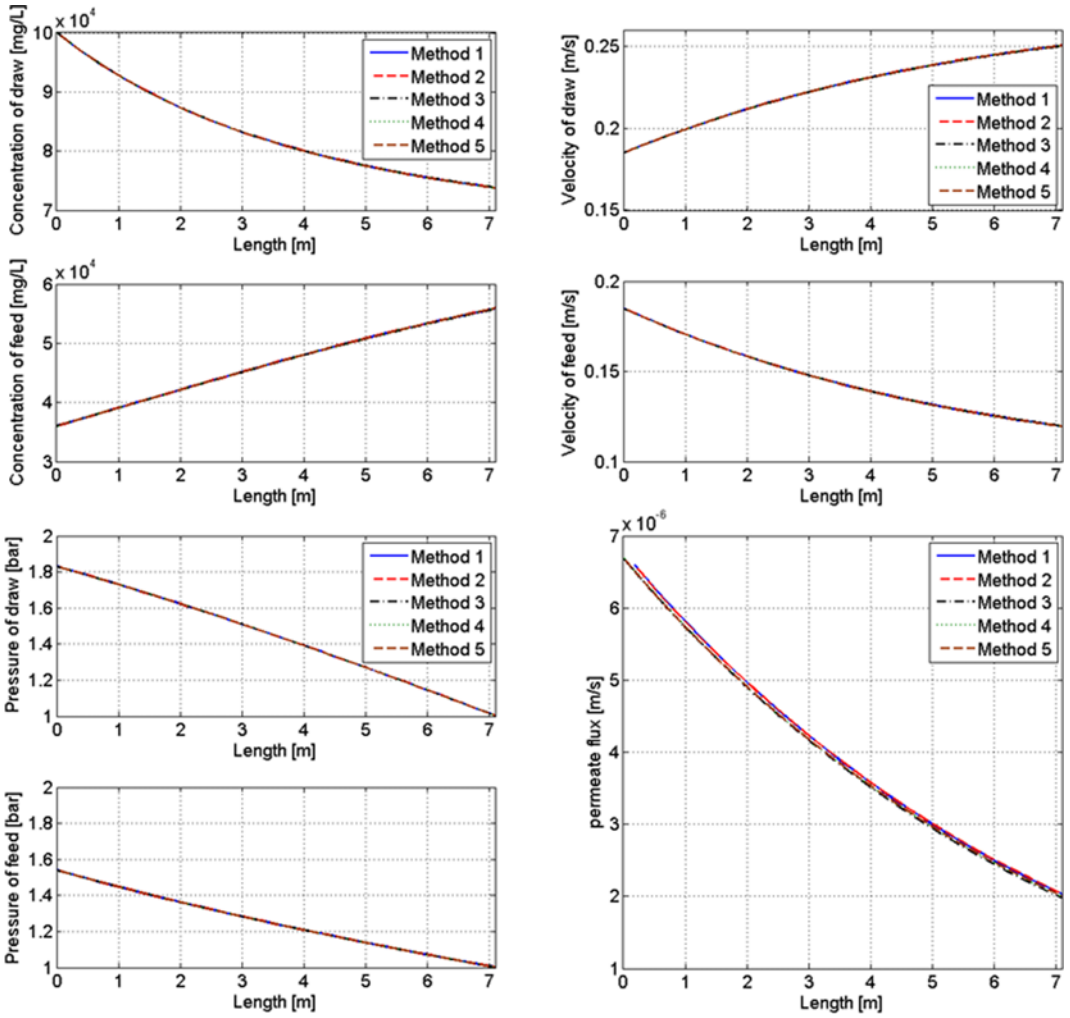

Fig. 8. Simulation results of the FO process along the flow direction.

Table 5. Computation times of the five methods

	RO process			FO process		
	Single [s]	X100 [s]	Ratio [%]	Single [s]	X100 [s]	Ratio [%]
Method 1	0.0078	0.8877	100.00	0.0100	1.1444	100.00
Method 2	0.0074	0.8701	98.01	0.0099	1.1147	97.40
Method 3	0.0231	2.2472	253.14	0.0300	2.9532	258.05
Method 4	0.0742	7.3352	826.28	0.1023	10.1121	883.59
Method 5	0.0698	6.8999	777.25	0.1001	9.9026	865.28

Table 6. Operating conditions for the robustness test

		RO	FO
Feed flow rate [m^3/day]	High	256780.8	256780.8
	Low	1283.9	1283.9
Driving force (RO: feed pressure, FO: concentration of draw solution)	High	100 [bar]	150 [kg/m^3]
	Low	40 [bar]	40 [kg/m^3]

4. Method 4 shows tolerable errors in accuracy, but its computation speed and robustness are poor.

5. Method 5 also shows tolerable errors in accuracy and robustness, but requires a long computation time.

From the results of three performance parameters, accuracy, computation time, and robustness, Method 2, using RK4 and a trans-

Table 7. Simulation results of the robustness test in the RO process

Axial velocity	High	High	Low	Low
Driving force	High	Low	High	Low
Method 1	Success	Success	**Fail**	Success
Method 2	Success	Success	Success	Success
Method 3	Success	Success	Success	Success
Method 4	Success	Success	**Fail**	Success
Method 5	Success	Success	Success	Success

Table 8. Simulation results of the robustness test in the FO process

Axial velocity	High	High	Low	Low
Driving force	High	Low	High	Low
Method 1	Success	Success	**Fail**	Success
Method 2	Success	Success	Success	Success
Method 3	**Fail**	Success	**Fail**	**Fail**
Method 4	Success	Success	**Fail**	Success
Method 5	Success	Success	Success	Success

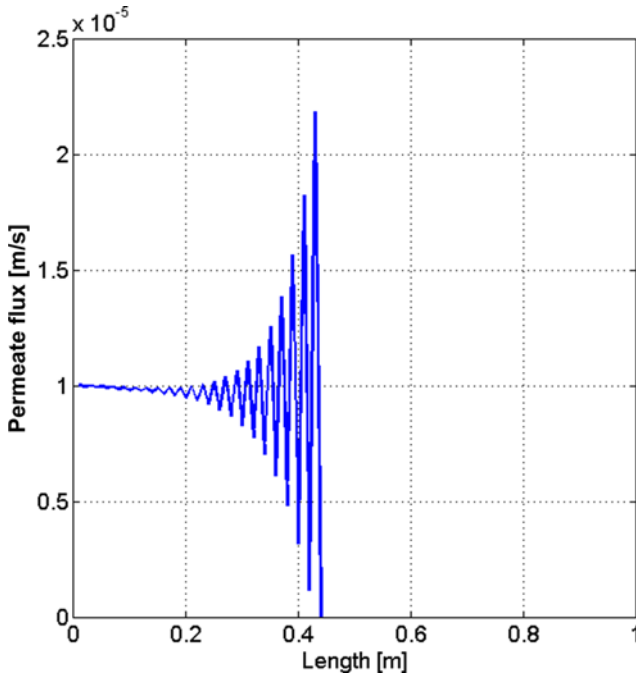

Fig. 9. Oscillation of water flux in Method 3.

formation to explicit equations, was found to display the best performance.

CONCLUSIONS

In the RO and FO processes, concentration polarization effects exist owing to membrane characteristics such as selectivity, permeability, and asymmetric structure. Generally, concentration polarization effects are taken into consideration by introducing exponential terms to express polarized concentrations. However, because of these exponential terms, the flux model becomes nonlinear and implicit, so that iterative procedures are required for calculations, which usually takes up large computation times. In this study, a method for transforming implicit equations to their explicit forms is suggested, in order to avoid the iterative procedure. In addition, the performance of five solving methods was tested and compared in terms of accuracy, computation time, and robustness based on input conditions. In conclusion, the method using the 4th order Runge-Kutta equation and transformation to the explicit form of equations shows the best performance. The transformation method presented in this study is, therefore, extremely robust in various simulation conditions, accurate, and has a cost-effective computation time.

ACKNOWLEDGEMENTS

This research was supported by a grant (07seaheroB02-01-01) from the Plant Technology Advancement Program funded by the Ministry of Land, Transport and Maritime Affairs of the Korean government.

REFERENCES

1. U. Merten, Desalination by reverse osmosis, M.I.T. Press, Cambridge (1966).
2. O. Kedem and A. Katchalsky, *Biochimica et Biophysica Acta*, **27**, 229 (1958).
3. K. S. Spiegler and O. Kedem, *Desalination*, **1**, 311 (1966).
4. G. Jonsson, *Desalination*, **24**, 19 (1978).
5. A. L. Zydney, *J. Membr. Sci*., **130**, 275 (1997).
6. S. Sundaramoorthy, G. Srinivasan and D. V. R. Murthy, *Desalination*, **280**, 403 (2011).
7. G. Srinivasan, S. Sundaramoorthy and D. V. R. Murthy, *Desalination*, **281**, 199 (2011).
8. S. Senthilmurugan, A. Ahluwalia and S. K. Gupta, *Desalination*, **173**, 269 (2005).
9. K. Jamal, M. A. Khan and M. Kamil, *Desalination*, **160**, 29 (2004).
10. H. Mehdizadeh, Kh. Molaiee-Nejad and Y. C. Chong, *J. Membr. Sci*., **267**, 27 (2005).
11. W. Zhou, L. Song and T. K. Guan, *J. Membr. Sci*., **271**, 38 (2006).
12. C. R. Bouchard, P. J. Carreau, T. Matsuura and S. Sourirajan, *J. Membr. Sci*., **97**, 215 (1994).
13. E. Lyster and Y. Cohen, *J. Membr. Sci*., **303**, 140 (2007).
14. A. I. C. Morão, A. M. B. Alves and V. Geraldes, *J. Membr. Sci*., **325**, 580 (2008).
15. S. Kim and E. M. V. Hoek, *Desalination*, **186**, 111 (2005).
16. V. Geraldes and M. D. Afonso, *J. Membr. Sci*., **300**, 20 (2007).
17. J. R. McCutcheon and M. Elimelech, *J. Membr. Sci*., **284**, 237 (2006).
18. B. Gu, D. Y. Kim, J. H. Kim, S. Lee and D. R. Yang, *J. Membr. Sci*., **379**, 403 (2011).
19. J. R. McCutcheon and M. Elimelech, *AIChE J*., **53**, 1736 (2007).
20. C. H. Tan and H. Y. Ng, *J. Membr. Sci*., **324**, 209 (2008).
21. G. R. Lindfield and J. E. T. Penny, *Numerical Methods*, 3rd Ed., Elsevier, 233 (2012).
22. M. Shacham and E. Kehat, *Chem. Eng. Sci*., **28**, 2187 (1973).
23. W. F. Ramirez, *Computational methods for process simulation*, 2nd Ed., Butterworth-Heinemann (1997).